6402 *Inorg. Chem.* **2010**, *49*, 6402–6408
DOI: 10.1021/ic902266x

Inorganic Chemistry
Article

Phosphorescence Imaging of Homocysteine and Cysteine in Living Cells Based on a Cationic Iridium(III) Complex

Liqin Xiong,[†] Qiang Zhao,[†] Huili Chen,*[,†,‡] Yanbo Wu,[‡] Zesheng Dong,[†] Zhiguo Zhou,[†] and Fuyou Li*[,†]

[†]*Department of Chemistry, Fudan University, Shanghai 200433, P.R. China, and* [‡]*Institute of Molecular Science, Key Laboratory of Chemical Biology and Molecular Engineering of Education Ministry, Shanxi University, Taiyuan 030006, P.R. China*

Received November 16, 2009

Homocysteine (Hcy) and cysteine (Cys) are crucial to the physiological balance in living systems. Specific detection of intracellular Hcy and Cys is of growing importance. Herein, we demonstrated phosphorescence imaging of intracellular Hcy and Cys using a cationic iridium(III) complex $Ir(pba)_2(bpy)^+ \cdot PF_6^-$ [pba = 4-(2-pyridyl)benzaldehyde, bpy = bipyridine] containing aldehyde groups as a luminescent probe. Upon addition of Hcy or Cys to a semiaqueous solution of $Ir(pba)_2(bpy)^+$, a change in luminescence from yellow to red was visible to the naked eye. The successful chemical reaction of the aldehyde in $Ir(pba)_2(bpy)^+$ with Hcy and Cys to form thiazinane and thiazolidine was confirmed by ^1H NMR. Moreover, complexation with Hcy and Cys disturbed the p-π conjugation between the aldehyde group and the bpy moiety, and led to the excited states switching to [dπ(Ir)-$\pi_{N\wedge N}$*] ^{3}MLCT and [$\pi_{C\wedge N}$-$\pi_{N\wedge N}$*] ^{3}LLCT from ($\pi-\pi$*)(pba^-) ^{3}IL. Furthermore, the MTT assay was used to determine that the probe has low cytotoxicity. Importantly, cell imaging experiments demonstrated that the probe is membrane permeable and can monitor the changes of Hcy/Cys within living cells in a ratiometric mode.

Introduction

Thiol-containing amino acids, homocysteine (Hcy) and cysteine (Cys), play many crucial roles in biological systems. The level of Hcy in plasma is an indicator of disorders including cardiovascular and Alzheimer's disease.[1] Cys deficiency is associated with slowed growth, hair depigmentation, edema, lethargy, liver damage, muscle and fat loss, skin lesions, and weakness.[2] Great attention has been paid to the detection of Hcy and Cys. In particular, there are recent reports of fluorescence probes for the specific detection of Hcy and Cys,[3−16] and most of the reported fluorescent probes are limited to detecting Hcy and Cys in solution. To date, only few examples of fluorescence turn-on probes have been reported for visualizing Hcy/Cys in cells by fluorescence microscopy.[11,15,16] For example, we previously described a fluorescent probe for imaging Hcy/Cys in cells with a 75-fold fluorescence enhancement.[11] Peng's group recently reported a fluorescent off-on chemodosimeter that can distinguish Cys from other amino acids in cells.[16] However, these works are limited to fluorescent detection based on organic dyes as probes. Compared with fluorescent dyes, phosphorescent iridium(III) complexes show some advantageous photophysical properties such as a relative long lifetime and high

*To whom correspondence should be addressed. Fax: 86-21-55664621. Phone: 86-21-55664185. E-mail: fyli@fudan.edu.cn (F.L.).

(1) Seshadri, S.; Beiser, A.; Selhub, J.; Jacques, P. F.; Rosenberg, I. H.; D'Agostino, R. B.; Wilson, P. W. F. *N. Engl. J. Med.* **2002**, *346*, 476.
(2) Shahrokhian, S. *Anal. Chem.* **2001**, *73*, 5972.
(3) Rusin, O.; Luce, N. N. S.; Agbaria, R. A.; Escobedo, J. O.; Jiang, S.; Warner, I. M.; Dawan, F. B.; Lian, K.; Strongin, R. M. *J. Am. Chem. Soc.* **2004**, *126*, 438.
(4) Tanaka, F.; Mase, N.; Barbas, C. F., III *Chem. Commun.* **2004**, 1762.
(5) Wang, W. H.; Rusin, O.; Xu, X. Y.; Kim, K. K.; Escobedo, J. O.; Fakayode, S. O.; Fletcher, K. A.; Lowry, M.; Schowalter, C. M.; Lawrence, C. M.; Fronczek, F. R.; Warner, I. M.; Strongin, R. M. *J. Am. Chem. Soc.* **2005**, *127*, 15949.
(6) Lu, C.; Zu, Y. B. *Chem. Commun.* **2007**, 3871.
(7) Lee, K. S.; Kim, T. K.; Lee, J. H.; Kim, H. J.; Hong, J. I. *Chem. Commun.* **2008**, 6173.
(8) Lin, W. Y.; Long, L. L.; Yuan, L.; Cao, Z. M.; Chen, B. B.; Tan, W. *Org. Lett.* **2008**, *10*, 5577.
(9) Kim, T. K.; Lee, D. N.; Kim, H. J. *Tetrahedron Lett.* **2008**, *49*, 4879.
(10) Zhang, X. J.; Ren, X. S.; Xu, Q. H.; Loh, K. P.; Chen, Z. K. *Org. Lett.* **2009**, *11*, 1257.
(11) Zhang, M.; Yu, M. X.; Li, F. Y.; Zhu, M. W.; Li, M. Y.; Gao, Y. H.; Li, L.; Liu, Z. Q.; Zhang, J.; Zhang, D. Q.; Yi, T.; Huang, C. H. *J. Am. Chem. Soc.* **2007**, *129*, 10322.
(12) Zhang, M.; Li, M. Y.; Zhao, Q.; Li, F. Y.; Zhang, D. Q.; Zhang, J. P.; Yi, T.; Huang, C. H. *Tetrahedron Lett.* **2007**, *48*, 2329.
(13) Chen, H. L.; Zhao, Q.; Wu, Y. B.; Li, F. Y.; Yang, H.; Yi, T.; Huang, C. H. *Inorg. Chem.* **2007**, *46*, 11075.
(14) Huang, K. W.; Yang, H.; Zhou, Z. G.; Chen, H. L.; Li, F. Y.; Yi, T.; Huang, C. H. *Inorg. Chim. Acta* **2009**, *362*, 2577.
(15) Duan, L. P.; Xu, Y. F.; Qian, X. H.; Wang, F.; Liu, J. W.; Cheng, T. Y. *Tetrahedron Lett.* **2008**, *49*, 6624.
(16) Li, H. L.; Fan, J. L.; Wang, J. Y.; Tian, M. Z.; Du, J. J.; Sun, S. G.; Sun, P. P.; Peng, X. J. *Chem. Commun.* **2009**, 5904.
(17) Yu, M. X.; Zhao, Q.; Shi, L. X.; Li, F. Y.; Zhou, Z. G.; Yang, H.; Yi, T.; Huang, C. H. *Chem. Commun.* **2008**, 2115.
(18) Zhao, Q.; Yu, M. X.; Shi, L. X.; Liu, S. J.; Li, C. Y.; Shi, M.; Zhou, Z. G.; Huang, C. H.; Li, F. Y. *Organometallics* **2010**, *29*, 1085.

Published on Web 06/21/2010

Scheme 1. Chemical Structure of Complex $Ir(pba)_2(acac)$ and **1**

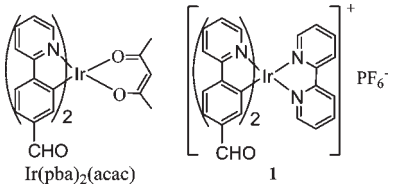

photostability, and some iridium complexes have been used as luminescent probes.[17−24] In a previous study, we reported the neutral iridium(III) complex $Ir(pba)_2(acac)$ (pba = 4-(2-pyridyl)benzaldehyde, acac = acetylacetonate, see Scheme 1)[13] as a selective phosphorescence turn-on probe for homocysteine over cysteine, by virtue of photoinduced electron transfer occurring in the adduct $Ir(pba)_2(acac)$-Cys from the thiazolidine group to the excited metal-to-ligand charge transfer (MLCT), resulting in weak photoluminescence of $Ir(pba)_2$-(acac)-Cys. Unfortunately, a high concentration (200 equiv) of Hcy is required, limiting its application. Moreover, in practical applications of these luminescence-enhanced probes, changes in luminescence intensity can also be caused by many other variable factors, such as probe molecule concentration, pH, polarity, temperature, and photobleaching.

In comparison with luminescence-enhanced detection, ratiometric measurement affords simultaneous recording of two emission intensities at different wavelengths in the presence and absence of analytes and thus provides built-in correction for environmental effects.[25−32] In this present study, the iridium-(III) complex $Ir(pba)_2(acac)$[13] was modified by replacing the ligand acetylacetonate with 2,2′-bipyridine, and a cationic iridium(III) complex $Ir(pba)_2(bpy)^+ \cdot PF_6^-$ (**1**, bpy = bipyridine, see Scheme 1)[33] containing the aldehyde groups was prepared as a novel Hcy/Cys-selective probe for ratiometric phosphorescence imaging in living KB cells. Our design strategy for the detection of Hcy/Cys is based on the selective reaction of aldehyde of the ligand pba with the β,γ-aminothiol group to form thiazolidine and thiazinane,[3,4,12−14] affecting the p-π conjugation between the aldehyde and the phenyl moiety, switching the excited states from $(\pi-\pi^*)(pba^-)$ ^{3}IL to $[d\pi(Ir)-\pi_{N^\wedge N}^*]$ ^{3}MLCT and $[\pi_{C^\wedge N}-\pi_{N^\wedge N}^*]$ ^{3}LLCT, resulting in a shift of phosphorescence emission of the iridium complex.[34,35]

Experimental Section

Materials. 4-(2-pyridyl)benzaldehyde (Hpba), bipyridine (bpy) and homocysteine (Hcy) were purchased from Acros. Other amino acids were purchased from Sinopharm Chemical Reagent Co., Ltd. (Shanghai). $IrCl_3 \cdot 3H_2O$ was an industrial product and used without further purification. **1** was synthesized according to the ref 33, and its structure was confirmed by NMR and MS spectra. ^{1}H NMR (400 MHz, DMSO, 25 °C): δ = 9.72 (s, 2H,13-H), 8.90 (d, $^3J_{H,H}$ = 8.0 Hz, 2H, 9-H), 8.48 (d, $^3J_{H,H}$ = 8.0 Hz, 2H, 1-H), 8.29 (d, $^3J_{H,H}$ = 8.0 Hz, 2H, 12-H), 8.19 (d, $^3J_{H,H}$ = 7.6 Hz, 2H, 4-H), 8.09 (dd, $^3J_{H,H}$ = 7.6 Hz 2H, 3-H), 7.86 (d, $^3J_{H,H}$ = 4.2 Hz, 2H, 5-H), 7.75 (d, $^3J_{H,H}$ = 4.2 Hz, 2H, 6-H), 7.68 (t, $^3J_{H,H}$ = 8.0 Hz, 2H, 10-H), 7.59 (t, $^3J_{H,H}$ = 8.0 Hz, 2H, 11-H),7.32 (d, $^3J_{H,H}$ = 8.0 Hz, 2H, 2-H), 6.66 (s, 2H, 8-H). Electrospray ionization MS (ESI-MS): m/z 713 (M^+).

Synthesis of 1-Hcy and 1-Cys. The mixture of **1** and Hcy (or Cys) was refluxed in ethanol and water (8:1, v/v) for 12 h. The crude product was purified on CombiFlash reversed-phase liquid chromatography (C18, 40 g). The mobile phase was changed from 10% methanol in water (10 mM NH_4HCO_3) to 38% methanol in water (10 mM NH_4HCO_3) in 20 min, and held at 38% for 20 min. The flow rate was 35 mL/min, and UV absorbance was monitored at 254 nm. The appropriate fractions were combined and evaporated in vacuo to give the product as a yellow solid. Analytical purity was assessed by analytical reversed-phase liquid chromatography: XBRIDGE-C18, 4.6 mm × 50 mm, 3.5 μm. The mobile phase was changed from 5% acetonitrile in water (10 mM NH_4HCO_3) to 95% acetonitrile in water (10 mM NH_4HCO_3) in 1.2 min. The flow rate was 1.8 mL/min and UV absorbance was monitored at 254 nm. **1**-Hcy and **1**-Cys were characterized by means of ^{1}H NMR, ^{13}C NMR (Supporting Information, Figures S1 and Figure S2), and HRMS (Supporting Information, Figures S3 and Figure S4).

1-Hcy, yield, 22%. ^{1}H NMR (400 MHz, CD_3OD): δ 8.65 (2H), 8.15 (4H), 8.03 (2H), 7.91 (2H), 7.83 (2H), 7.65 (2H), 7.49 (2H), 7.21 (4H), 6.36 (2H), 4.87 (2H), 3.26 (2H), 3.13 (2H), 2.78 (2H), 2.13 (2H), 1.50 (2H). MS (m/z) calcd. for $IrC_{42}H_{38}N_6O_4S_2$ 947.20; found 947.20 (M^+).

1-Cys, yield, 18%. ^{1}H NMR (400 MHz, CD_3OD): δ 8.70 (2H), 8.18 (4H), 8.04 (2H), 7.89 (4H), 7.68 (2H), 7.57 (2H), 7.23 (2H), 7.12 (2H), 6.42 (2H), 5.16 (2H), 3.62 (2H), 2.92 (4H). MS (m/z) calcd. for $IrC_{40}H_{34}N_6O_4S_2$ 919.17; found 919.17(M^+).

General Experiments. ^{1}H NMR spectra were recorded on a Varian spectrometer at 400 MHz. Electrospray ionization mass spectra (ESI-MS) were measured on a Micromass LCTTM system. The UV−visible spectra were recorded on a Shimadzu UV-2550 spectrometer. Steady-state emission experiments at room temperature were measured on an Edinburgh Instruments LFS-920 spectrometer. Lifetime studies were performed with an Edinburgh FLS 920 photocounting system with a hydrogen-filled lamp as the excitation source. The data were analyzed by iterative convolution of the luminescence decay profile with the instrument response function using a software package provided by Edinburgh Instruments.

Amino Acids Titration of 1. Spectrophotometric determination was performed in DMSO-HEPES buffer (pH 7.2, 9:1 v/v). Aliquots of stock solutions of amino acid were titrated into a solution of **1** in DMSO-HEPES buffer. The tubes were kept at 37 °C overnight before the UV−vis absorption and fluorescent spectra of the samples were recorded.

Cell Culture. The human nasopharyngeal epidermal carcinoma cell line (KB cells) was provided by the Institute of Biochemistry and Cell Biology, SIBS, CAS (China). The KB cells were grown in RPMI 1640 (Roswell Park Memorial Institute's Medium) supplemented with 10% FBS (Fetal Bovine Serum)

(19) Jiang, W. L.; Gao, Y.; Sun, Y.; Ding, F.; Xu, Y.; Bian, Z. Q.; Li, F. Y.; Bian, J.; Huang, C. H. *Inorg. Chem.* **2010**, *49*, 3252.
(20) Lo, K. K. W.; Lee, P. K.; Lau, J. S. Y. *Organometallics* **2008**, *27*, 2998.
(21) Zhang, K. Y.; Lo, K. K. W. *Inorg. Chem.* **2009**, *48*, 6011.
(22) Lau, J. S. Y.; Lee, P. K.; Tsang, K. H. K.; Ng, C. H. C.; Lam, Y. W.; Cheng, S. H.; Lo, K. K. W. *Inorg. Chem.* **2009**, *48*, 708.
(23) Zhang, K. Y.; Li, S. P. Y.; Zhu, N. Y.; Or, I. W. S.; Cheung, M. S. H.; Lam, Y. W.; Lo, K. K. W. *Inorg. Chem.* **2010**, *49*, 2530.
(24) Zhao, Q.; Li, F. Y.; Huang, C. H. *Chem. Soc. Rev.* **2010**, DOI: 10.1039/B915340C.
(25) Maruyama, S.; Kikuchi, K.; Hirano, T.; Urano, Y.; Nagano, T. *J. Am. Chem. Soc.* **2002**, *124*, 10650.
(26) Taki, M.; Wolford, J. L.; O'Halloran, T. V. *J. Am. Chem. Soc.* **2004**, *126*, 712.
(27) Jares-Erijman, E. A.; Jovin, T. M. *Nat. Biotechnol.* **2003**, *21*, 1387.
(28) Sapsford, K. E.; Berti, L.; Medintz, I. L. *Angew. Chem., Int. Ed.* **2006**, *45*, 4562.
(29) Levitt, J. A.; Matthews, D. R.; Ameer-Beg, S. M.; Suhling, K. *Curr. Opin. Biotechnol.* **2009**, *20*, 28.
(30) Xu, Z. C.; Xiao, Y.; Qian, X. H.; Cui, J. N.; Cui, D. W. *Org. Lett.* **2005**, *7*, 889.
(31) Xu, Z. C.; Qian, X. H.; Cui, J. N. *Org. Lett.* **2005**, *7*, 3029.
(32) Liu, B.; Tian, H. *Chem. Commun.* **2005**, 3156.
(33) Lo, K. K. W.; Chung, C. K.; Zhu, N. *Chem.—Eur. J.* **2003**, *9*, 475.
(34) Lo, K. K. W.; Chung, C. K.; Zhu, N. *Chem.—Eur. J.* **2006**, *12*, 1500.
(35) Lo, K. K. W.; Zhang, K. Y.; Chung, C. K.; Kwok, K. Y. *Chem.—Eur. J.* **2007**, *13*, 7110.

at 37 °C and 5% CO_2. Cells (5×10^8/ L) were plated on 14 mm glass coverslips and allowed to adhere for 24 h.

Cytotoxicity Assay. The in vitro cytotoxicity was measured using the methyl thiazolyl tetrazolium (MTT) assay in human nasopharyngeal epidermal carcinoma cell line KB. Cells growing in log phase were seeded into a 96-well cell-culture plate at 1×10^4/well and then incubated for 24 h at 37 °C under 5% CO_2. Compound **1** (100 μL/well) at concentrations of 5, 25, 50, 100 μM was added to the wells of the treatment group, and 100 μL/well DMSO diluted in RPMI 1640 at final concentration of 0.2% to the negative control group, respectively. The cells were incubated for 24 h at 37 °C under 5% CO_2. Subsequently, 10 μL MTT (5 mg/mL) was added to each well of the 96 well assay plate and incubated for an additional 4 h at 37 °C under 5% CO_2. After the addition of 10% sodium dodecyl sulfate (SDS, 100 μL/well), the assay plate was allowed to stand at room temperature for 12 h. A Tecan Infinite M200 monochromator-based multifunction microplate reader was used to measure the OD570 (A value) of each well with background subtraction at 690 nm. The following formula was used to calculate the viability of cell growth:

$$\text{cell viability}(\%) = (\text{mean of Absorbance value of treatment group}/\text{mean of Absorbance value of control}) \times 100$$

Confocal Luminescence Imaging. Confocal luminescence imaging of cells was performed with an OLYMPUS FV1000 laser scanning microscope, and a 60× oil-immersion objective lens was used. The KB cells incubated with **1** were excited with a semiconductor laser at 405 nm, and emission was collected at 530 ± 10 and 570 ± 10 nm.

Energy Optimization.[13] The geometric and energy optimizations were performed with the Gaussian 03 program based on the density functional theory (DFT) method. The Becke's three-parameter hybrid functional with the Lee−Yang−Parr correlation functional (B3LYP) was employed for all the calculations. The LANL2DZ basis set was used to treat the iridium atom, whereas the 3-21G* basis set was used to treat all other atoms. Once an optimized geometry was obtained, imaginary frequencies were checked at the same level by vibration analysis to verify the genuine minimum on the potential energy surfaces (PES). To understand the nature of the excited state, the orbital analyses of the complexes were also performed.

Results and Discussion

Photophysical Properties of 1, 1-Hcy, and 1-Cys. The absorption and emission spectra of **1**, **1**-Hcy, and **1**-Cys were investigated in DMSO-HEPES buffer (pH 7.2, 9:1 v/v). As shown in Figure 1, complex **1** has intense absorption bands in the ultraviolet region 280−380 nm, with an extinction coefficient ε of $\sim 10^5$ mol$^{-1}\cdot$L$\cdot$cm^{-1}, assigned to spin-allowed singlet ligand-centered (^{1}LC) transitions. The weak band at ~430 nm with ε of $\sim 10^3$ mol$^{-1}\cdot$L$\cdot$cm^{-1} is assigned to a metal-to-ligand charge transfer (MLCT) transition.[33−37] Clearly, the maximal absorption wavelength $\lambda_{max}{}^{abs}$ = 430 nm of **1** is red-shifted in comparison to that of complex **1**-Hcy/**1**-Cys with $\lambda_{max}{}^{abs}$ = 410 nm (Supporting Information, Figure S5), which is attributed to the introduction of an aldehyde group into **1**.

In DMSO-HEPES buffer (pH 7.2, 9:1 v/v), **1** displays a structural emission band with maximal wavelength at 547 nm and a shoulder at 586 nm (Figure 1). Moreover,

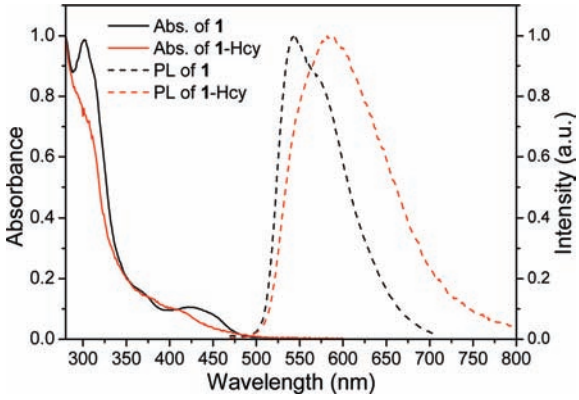

Figure 1. Absorption and emission spectra of **1** and **1**-Hcy (20 μM) in DMSO-HEPES buffer (pH 7.2, 9:1 v/v).

the emission lifetime monitored at 547 nm in an air-equilibrated solution at room temperature was 691 ns. The structural emission of **1**, along with the longer lifetime, and the absence of a significant blue-shift in the emission wavelength upon lowering the temperature from 298 to 77 K (Supporting Information, Figure S6) suggest that the excited state of **1** has ($\pi-\pi^*$)(pba$^-$) ^{3}IL character, with mixing of a small quantity of [dπ(Ir)-π^*(pba$^-$)] ^{3}MLCT. However, complex **1**-Hcy/**1**-Cys exhibited a broad and structureless emission band with a maximal emission wavelength at 586 nm (Supporting Information, Figure S6). Moreover, a notable blue-shift was observed at 77 K, which is attributed to the [dπ(Ir)-$\pi_{C\wedge N}$*] ^{3}MLCT and [dπ(Ir)-$\pi_{N\wedge N}$*] ^{3}MLCT. Moreover, the quantum efficiency in DMSO-HEPES buffer (pH 7.2, 9:1 v/v) was 0.0188 for **1**-Hcy and 0.019 for **1**-Cys with reference to quinine sulfate as a standard. The emission lifetimes monitored at 586 nm in an air-equilibrated solution at room temperature are 213 and 184 ns for **1**-Hcy and **1**-Cys, respectively. Such long lifetimes in an air-equilibrated solution show that the emitting states of **1**-Hcy and **1**-Cys also have triplet character. As expected, the introduction of an aldehyde group causes blue-shift of the maximal emission wavelength for **1**, indicating that the aldehyde group is an important contributor to the photophysical properties of **1**. Only Cys and Hcy have the characteristic structure of the β,γ-aminothiol group among the amino acids and peptides. Therefore, it can be expected that **1** containing the aldehyde groups could be used as a selectively luminescent probe for Cys/Hcy with red-shift emission.

Response of 1 to Hcy and Cys. (a). ^{1}H NMR Spectra. The ^{1}H NMR interaction of **1** with Hcy/Cys was investigated, and the results are shown in Figure 2. When excess Hcy or Cys was added to a solution of **1** in DMSO-d_6, the aldehyde resonance (9.73 ppm) of **1** disappeared, and a new peak at ~5 ppm, assigned to the methine proton of the thiazinane or thiazolidine diastereometer,[3] was observed. With the disappearance of the strong electron-withdrawing group (CHO), the resonances corresponding to the phenyl group shifted upfield. These facts indicate that thiazinane (or thiazolidine) was formed by the interaction of aldehyde with Hcy (or Cys), as shown in Scheme 2.

(b). UV−vis Absorption and Phosphorescence Spectra. The detection of Hcy and Cys by **1** was examined using a

(36) Liu, Z. W.; Bian, Z. Q.; Bian, J.; Li, Z. D.; Nie, D. B.; Huang, C. H. *Inorg. Chem.* **2008**, *47*, 8025.
(37) Chou, P. T.; Chi, Y. *Chem.—Eur. J.* **2007**, *13*, 380.

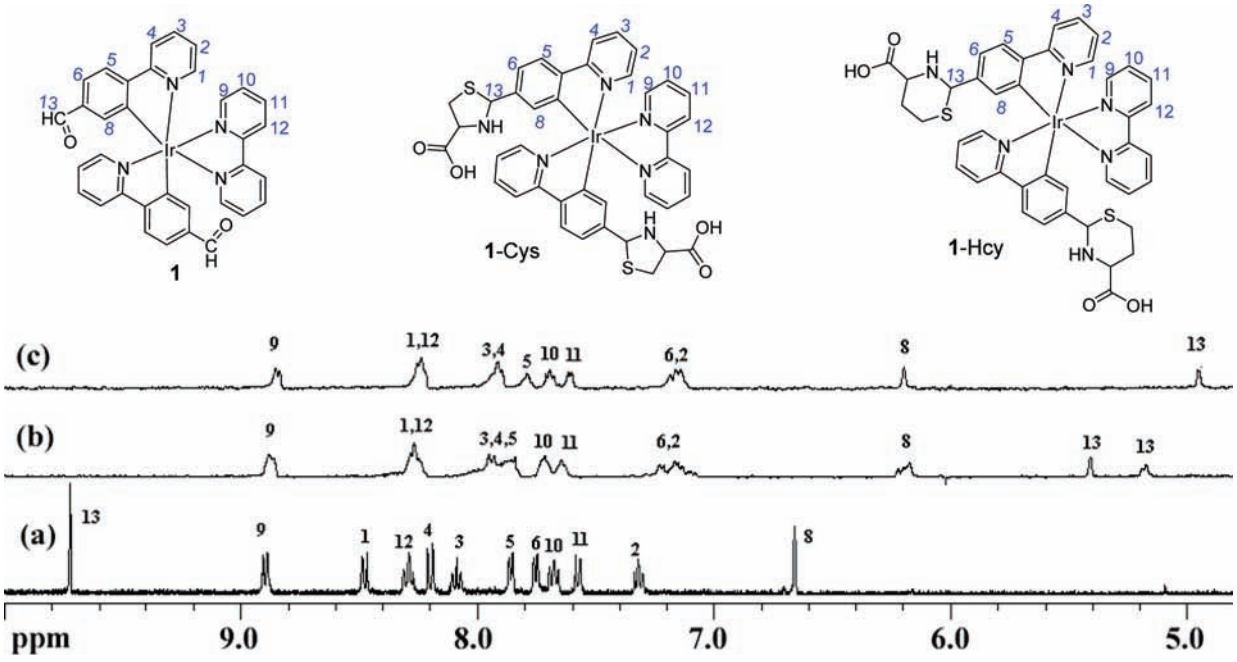

Figure 2. ^{1}H NMR spectra of **1** (a), **1**-Cys (b), and **1**-Hcy (c) in DMSO-d_6.

Scheme 2. Chemical Mechanism of **1** with Cys and Hcy

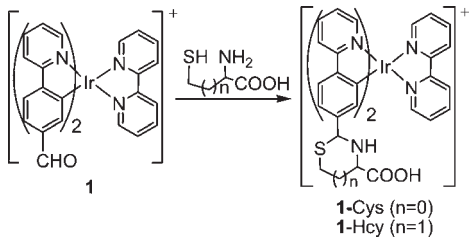

spectrophotometric method. As shown in Figure 3, upon addition of increasing amounts of Hcy (or Cys) to a solution of **1**, the absorbance at 435 and 301 nm decreased gradually whereas the absorbance at 390 nm increased, corresponding to a λ_{max} ^{abs} blue-shift of 45 nm with isosbestic points at 374 and 413 nm. Moreover, upon addition of Hcy (or Cys), the emission band progressively shifted to 586 nm with a decrease in intensity, corresponding to a red-shift of ~40 nm and a change in color from yellow to red, as shown in Figure 4. These facts indicate that the phosphorescent iridium complex **1** could serve as a "naked-eye" indicator of Hcy/Cys.

Mechanism of 1 in Sensing Hcy and Cys. Calculations based on density functional theory (DFT) for **1**, **1**-Hcy and **1**-Cys were done to further understand the high selectivity of **1** for detecting Hcy/Cys. The distributions of molecular orbitals (HOMO-2, HOMO-1, HOMO, LUMO, LUMO+1, and LUMO+2) are given in Table 1. For **1**, HOMO, HOMO-1 and HOMO-2 reside primarily at the iridium center and the phenyl part of the cyclometalated ligands, which is similar to most iridium(III) complexes.[38,39]

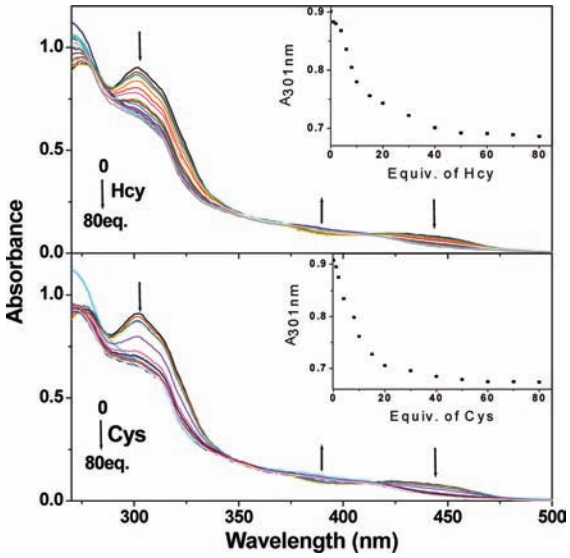

Figure 3. Changes in UV−vis absorption spectra of **1** (20 μM) in DMSO-HEPES buffer (pH 7.2, 9:1 v/v) with various amounts of Hcy or Cys (0−80 equiv). Inset: titration curves of **1** with Hcy or Cys.

The lowest unoccupied molecular orbital (LUMO) resides primarily on the bipyridine ligand, while LUMO+1 and LUMO+2 are localized mainly on the C^N ligand. Therefore, the HOMO (HOMO-1 and HOMO-2) →LUMO+1 (LUMO+2) transitions could contribute to the ^{3}IL($\pi-\pi^*$) (pba^-) excited state, with mixing of a small quantity of [dπ(Ir)-π_{N^N}*] ^{3}MLCT or [π_{CAN}-π_{N^N}*] ^{3}LLCT (HOMO→LUMO). For **1**-Hcy and **1**-Cys, the highest occupied molecular orbital (HOMO) and HOMO-1 are located partially on one thiazolidine ring. LUMO, LUMO+1 and LUMO+2 reside on the bipyridine ligand, which indicates that their emission is derived mainly from the [π_{C^N}-π_{N^N}*] ^{3}LLCT and [dπ(Ir)-π_{N^N}*] ^{3}MLCT. Furthermore, the corresponding energy gaps between HOMO and LUMO are calculated to be 2.86, 2.22, and 2.28 eV for **1**, **1**-Hcy, and **1**-Cys,

(38) Hwang, F. M.; Chen, H. Y.; Chen, P. S.; Liu, C. S.; Chi, Y.; Shu, C. F.; Wu, F. I.; Chou, P. T.; Peng, S. M.; Lee, G. H. *Inorg. Chem.* **2005**, *44*, 1344.

(39) Li, J.; Djurovich, P. I.; Alleyne, B. D.; Yousufuddin, M.; Ho, N. N.; Thomas, J. C.; Peters, J. C.; Bau, R.; Thompson, M. E. *Inorg. Chem.* **2005**, *44*, 1713.

respectively, which is in agreement with the remarkable red-shift in luminescence spectra of **1**-Hcy (Cys) compared with that of **1**. Therefore, upon addition of Hcy/Cys to a solution of **1**, the excited states switch to [dπ(Ir)-$\pi_{N^\wedge N}$*] ^{3}MLCT and [$\pi_{C^\wedge N}$-$\pi_{N^\wedge N}$*] ^{3}LLCT from ($\pi-\pi$*)(pba$^-$) ^{3}IL.

Comparison of Complex Ir(pba)$_2$(acac) and Complex 1 As to Their Response to Hcy and Cys. Although Ir(pba)$_2$-(acac) and complex **1** have the same C^N ligand pba and recognition site for the aldehyde group, they show differing responses to Hcy and Cys. To reach saturation, addition of ~40 equiv and ~200 equiv of Hcy and Cys is required for Ir(pba)$_2$(acac) and complex **1**, respectively. However, compared with Ir(pba)$_2$(acac), complex **1** shows low selectivity and response to both Hcy and Cys. It appears that the response mechanism of complex **1** is different from that of Ir(pba)$_2$(acac)[13] for sensing Hcy and Cys. For Ir(pba)$_2$(acac), the excited state is always fixed on the cyclometalated C^N ligand whether in the presence or absence of Hcy (or Cys). For complex **1**, the excited states switch from ($\pi-\pi$*)(pba$^-$) ^{3}IL to [dπ(Ir)-$\pi_{N^\wedge N}$*] ^{3}MLCT and [$\pi_{C^\wedge N}$-$\pi_{N^\wedge N}$*] ^{3}LLCT, resulting in its

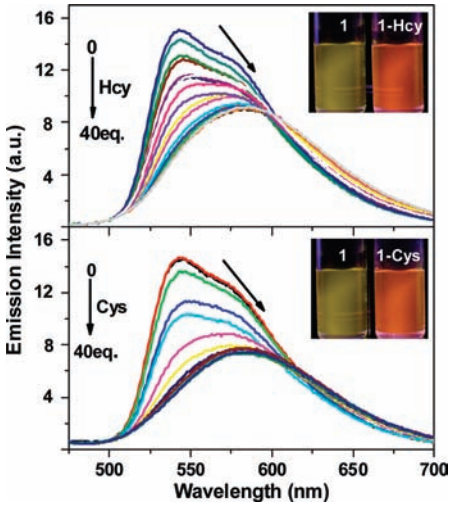

Figure 4. Changes in phosphorescence emission spectra of **1** (20 μM) in DMSO-HEPES buffer (pH 7.2, 9:1 v/v) upon addition of various amounts of Hcy or Cys (0−40 equiv) (λ_{ex} = 360 nm). Inset: Photos of photoluminescent emission of **1** in the absence or presence of 40 equiv of Hcy or Cys.

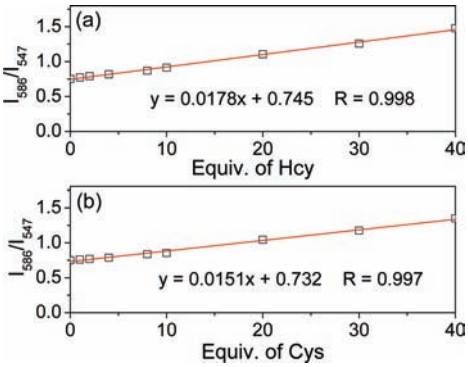

Figure 5. Plots of ratio I_{586}/I_{547} of luminescence intensity at 586 to 547 nm versus various amounts of Hcy/Cys (0−40 equiv) in DMSO-HEPES buffer (pH 7.2, 9:1 v/v).

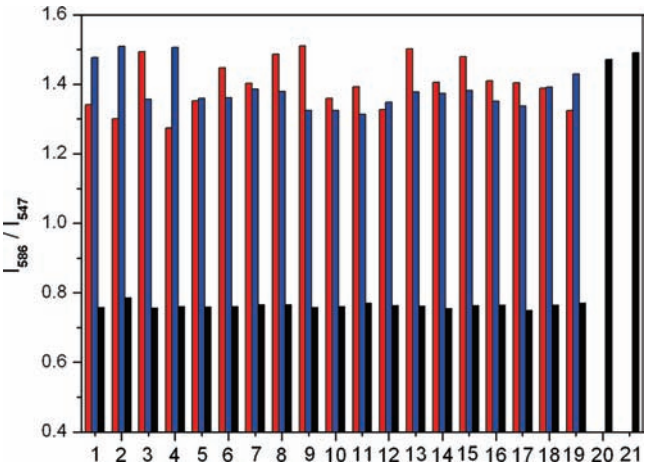

Figure 6. Luminescent responses of **1** (20 μM) in DMSO-HEPES buffer (pH 7.2, 9:1 v/v) to various amino acids (40 equiv) at 25 °C. Bars represent the ratio I_{586}/I_{547} of luminescence intensity at 586 to 547 nm. Black bars represent the addition of 40-fold various amino acids to a 20 μM solution of **1**. Blue and red bars represent the addition of Cys and Hcy (40 equiv) to the above solution, respectively. (λ_{ex} = 360 nm). 1, Ala; 2, Arg; 3, Asn; 4, Gln; 5, Glu; 6, Gly; 7, GSH; 8, His; 9, Ile; 10, Leu; 11,Lys; 12, Met; 13, Phe; 14, Pro; 15, Ser; 16, Thr; 17, Trp; 18, Tyr; 19, Val; 20, Cys; 21, Hcy.

Table 1. HOMO and LUMO Distributions of **1**, **1**-Cys, and **1**-Hcy

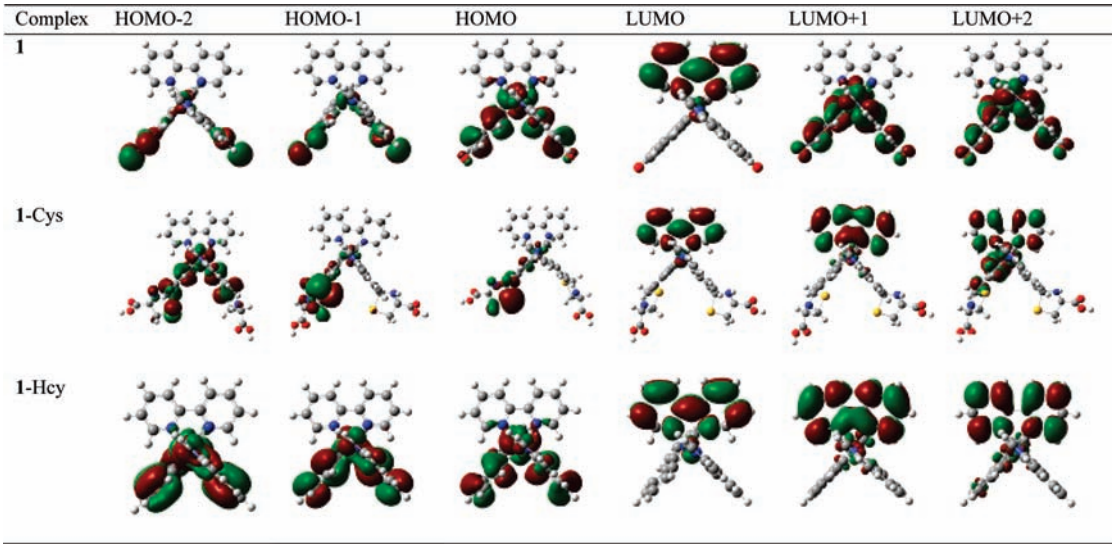

distinctive phosphorescent response, that may be applied in ratiometric measurement. Furthermore, when complex **1** (20 μM) and Hcy/Cys (0−40 equiv) were mixed in DMSO-HEPES buffer (pH 7.2, 9:1 v/v), the luminescence was measured. As shown in Figure 5, the concentration of Hcy and Cys in the range of 0−40 equiv was well correlated with the ratio (I_{586}/I_{547}) of luminescence intensity at 586 to 547 nm, indicating that complex **1** can be used in quantitative detection of Hcy and Cys concentrations.

Selective Optical Response of 1 to Various Amino Acids. Photoluminescent spectroscopy studies of the selective response of **1** have been extended to other elementary amino acids. Amino acids such as L-histidine, L-leucine, L-asparagine, L-arginine, L-tyrosine, L-threonine, L-proline, L-isoleucine, L-tryptophane, L-methionine, L-valine, L-alanine, L-phenylalanine, L-glutamine, L-glutamic acid, L-serine, L-lysine, and L-glycine did not produce detectable spectral changes (Figure 6). Even when structurally related thiol peptide (such as reduced glutathione, GSH) was served likewise, no spectral response in absorption and photoluminescence emission was observed, indicating that the formation of thiazolidine and thiazinane was a key for the selective recognition of Cys and Hcy. Notably, as shown in Figure 6, only the addition of Hcy or Cys caused an obvious red-shift emission at 586 nm. This visible emission allows Hcy and Cys to be distinguished from other amino acids by the naked eye. Furthermore, competition experiments with Hcy (or Cys) mixed with other amino acids showed no significant change in the ratio of luminescent intensity (I_{586}/I_{547}). These results show that **1** can be used to detect Hcy/Cys specifically.

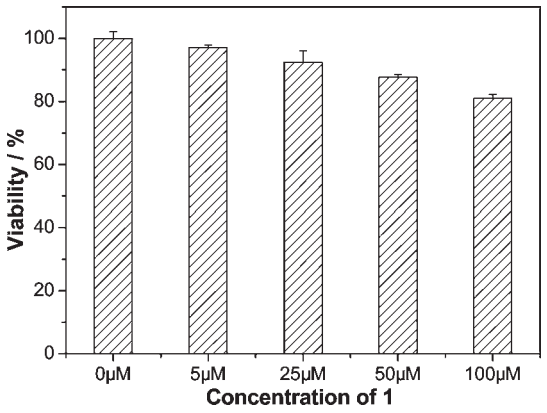

Figure 7. Cell viability values (%) estimated by an MTT proliferation test versus incubation concentrations of **1**. KB cells were cultured in the presence of 5−100 μM **1** at 37 °C for 24 h.

Cytotoxicity. To investigate the cytotoxicity of **1**, an MTT [3-(4,5-dimethylthiazol-2-yl)-2,5-diphenyltetrazolium bromide] assay with the human nasopharyngeal epidermal carcinoma cell line (KB cells) was used to determine the effect of **1** on cell proliferation after 24 h. No significant differences in the proliferation of the cells were observed in the absence or presence of 5−100 μM **1** (Figure. 7). The cellular viability was estimated to be greater than 80% after 24 h. These data show that **1** ($\leq$100 μM) can be considered to have low cytotoxicity.

Cell Imaging. We then tested the ability of **1** to monitor Hcy/Cys within living cells by confocal ratiometric phosphorescence imaging. The optical windows at the green channel (530 ± 10 nm) and red channel (570 ± 10 nm) were chosen as two signal outputs for ratiometric detection. For the adequate interaction between **1** and intracellular Hcy/Cys, the reaction was allowed to proceed at 37 °C for 30 min. As shown in Figure 8, KB cells incubated with 20 μM **1** for 30 min at 37 °C showed an

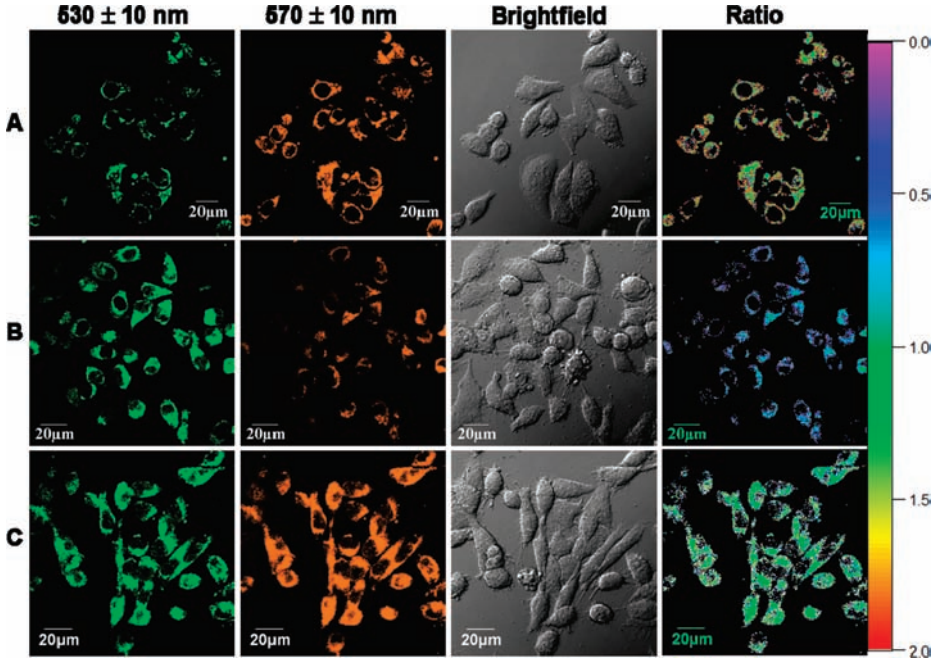

Figure 8. Ratio phosphorescence images of **1** in KB cells. (A), KB cells incubated with 20 μM **1** for 30 min. (B), KB cells incubated with 200 μM *N*-ethylmaleimide for 1 h and then further incubated with 20 μM **1** for 30 min. (C), KB cells incubated with 200 μM *N*-ethylmaleimide for 1 h and then further incubated with 20 μM **1** for 1 h. Emission was collected by the green channel from 530 ± 10 nm and red channel from 570 ± 10 nm (λ_{ex} = 405 nm). Ratio of emission intensity at 570 ± 10 nm to 530 ± 10 nm is also shown.

emission ratio of >1.5 at 570 ± 10 and 530 ± 10 nm (Figure 8A). The emission spectrum of living cells showed that the emission peak was located at ~570 nm (Supporting Information, Figure S7A), indicating the reaction of **1** with Hcy/Cys. Furthermore, the specific reaction of **1** with Hcy/Cys was further confirmed by a competition assay. The KB cells were preincubated with 200 μM *N*-ethylmaleimide (as a thio-reactive compound) at 37 °C for 1 h and then incubated with **1** at 37 °C for 30 min. As a result, the phosphorescence intensity of the green channel increased and that of the red channel decreased, so the ratio was reduced to <0.75 at 570 ± 10 and 530 ± 10 nm (Figure 8B). Moreover, emission spectra of living cells revealed that an obvious blue-shift of ~40 nm occurred (Supporting Information, Figure S7), which was consistent with the result obtained with DMSO-HEPES buffer. It should be stated that the phosphorescence intensity of the red channel increased slightly, with the incubation time of **1** increased to 1 h after preincubation with *N*-ethylmaleimide, and the ratio at 570 ± 10 and 530 ± 10 nm slowly changed to ~1 (Figure 8C and Supporting Information, Figure S7C), indicating the appearance of new Hcy/Cys in living KB cells and further reaction of **1** with the new Hcy/Cys. These facts suggest that **1** is cell-permeable and could be used for monitoring the changes of Hcy/Cys concentration within living cells.

Conclusions

In conclusion, we have described a cationic iridium(III) complex as a ratiometric phosphorescence probe for intracellular Hcy and Cys with an emission red-shift. This complex specifically responds to Hcy and Cys with a change in phosphorescence that is visible to the naked eye. ^{1}H NMR studies confirmed the formation of thiazinane (or thiazolidine) derived from the reaction of the aldehyde in the complex with Hcy (or Cys). Complexation with Hcy and Cys disturbed the p-π conjugation between the aldehyde and the fluorophor moiety of the iridium complex, resulting in the excited states switching to [dπ(Ir)-$\pi_{N\wedge N}$*] ^{3}MLCT and [$\pi_{C\wedge N}$-$\pi_{N\wedge N}$*] ^{3}LLCT from ($\pi-\pi$*)(pba$^-$) ^{3}IL. Furthermore, the MTT assay determined that the complex has low cytotoxicity. In particular, cell imaging experiments demonstrate that the complex is membrane-permeable and can readily reveal changes in intracellular Hcy/Cys concentration in a ratiometric way. It should be noted that the sensing of Cys and Hcys described in this work is not practicable because of the high concentrations of amino acid required and the resulting low sensitivity. However, this is a competent report of some interesting chemistry and may well be of interest to others working in the areas of molecular recognition and luminescent molecular reporters.

Acknowledgment. The authors thank National Natural Science Funds for Distinguished Young Scholars (20825101), and Shanghai Sci. Tech. Comm. (1052 nm03400), NCET-06-0353, Shanghai Leading Academic Discipline Project (B108), and the CAS/SAFEA International Partnership Program for Creative Research Teams for financial support.

Supporting Information Available: The absorption and emission spectra of **1**, **1**-Hcy, and **1**-Cys in CH_3OH at 77 K and 298 K; emission spectra obtained from living KB cells. This material is available free of charge via the Internet at http://pubs.acs.org.